Switchable Fluorescent Organogels and Mesomorphic Superstructure Based on Naphthalene Derivatives

ARTICLE *in* LANGMUIR · AUGUST 2007

Impact Factor: 4.46 · DOI: 10.1021/la7005919 · Source: PubMed

8 AUTHORS, INCLUDING:

Hong Yang
University of California, Los Angeles
255 PUBLICATIONS **7,262** CITATIONS
SEE PROFILE

Miao Xu
University of Utah
16 PUBLICATIONS **544** CITATIONS
SEE PROFILE

Chunhui Huang
Tamkang University
222 PUBLICATIONS **9,207** CITATIONS
SEE PROFILE

Switchable Fluorescent Organogels and Mesomorphic Superstructure Based on Naphthalene Derivatives

Hong Yang, Tao Yi,* Zhiguo Zhou, Yifeng Zhou, Juncheng Wu, Miao Xu, Fuyou Li,* and Chunhui Huang

Department of Chemistry & Laboratory of Advanced Materials, Fudan University, Shanghai 200433, People's Republic of China

Received March 1, 2007. In Final Form: May 14, 2007

Bisurea-functionalized naphthalene organogelators via cooperative hydrogen bonding and $\pi-\pi$ stacking interaction were designed and synthesized. The gelators showed excellent gelling capability in various solvents and performed switchable fluorescence in the gel state. The fluorescent emission of these compounds strongly depends on the aggregation of the fluorophore and is very sensitive to the temperature and chemical stimuli. A stronger and red-shifted emission was found in the gel state compared with the original solution. The gel−sol transition of the systems, as well as the fluorescent emission, is reversibly controlled by a change of the temperature or upon alternative addition of fluoride anions and protons. The influence of fluoride anions on the fluorescence and gel−sol processes is a result of the dissociation of intermolecular hydrogen bonds by bonding of fluoride anions with urea groups of the gelator. The obtained sol is turned to the gel state again upon addition of trifluoroacetic acid. Furthermore, polaring optical microscopy and small-angle X-ray scattering indicated that the gelator exhibited the liquid crystalline property and displayed the column phase.

Introduction

The self-assembly of small functional molecules into supramolecular structures is a powerful approach toward the development of new nanoscale materials and devices.[1] As a novel class of self-assembled materials, low weight molecular (LWM) gels organized in regular nanoarchitectures through specific noncovalent interactions including hydrogen bonds, hydrophobic interaction, $\pi-\pi$ interactions, and van der Waals forces have recently received considerable attention.[2] In particular, smart organogelators are of much interest for their potential applications such as in organic light emission diodes (OLEDs),[3] photovoltaic cells,[4] drug delivery,[5] and light harvesting systems.[6] Moreover, the formation and properties of these supramolecular gels can possibly be controlled by environmental stimuli such as light,[7] sound,[8] electrochemical stimuli,[9] complexation,[10] pH,[11] fluoride anions,[12] and a combination of some of these[13] by incorporating a receptor unit or a photoactive unit as a part of the gelator molecule.[14−17] For example, Shinkai et al. studied the influence of protons on the fluorescent properties of a 1,10-phenanthroline-appended cholesterol gelator.[18] Tian et al. constructed a multiple switching system responding to light, thermal stimuli, fluoride anions, and protons by using a photochromic fluorescent organogel based on bisthienylethene-bridged naphthahalimides.[19] Aida et al. reported a novel phosphorescent organogel from trinuclear gold(I) pyrazolate complex and studied the luminescent

* To whom correspondence should be addressed. E-mail: yitao@fudan.edu.cn (T.Y.); fyli@fudan.edu.cn (F.L.).

(1) (a) Terech, P.; Weiss, R. G. *Chem. Rev.* **1997**, *97*, 3133−3160. (b) van der Laan, S.; Feringa, B. L.; Kellogg, R. M.; van Esch, J. *Langmuir* **2002**, *18*, 7136−7140. (c) Deindorfer, P.; Geiger, T.; Schollmeyer, D.; Ye, J. H.; Zentel, R. *J. Mater. Chem.* **2006**, *16*, 351−358. (d) Estroff, L. A.; Hamilton, A. D. *Chem. Rev.* **2004**, *104*, 1201−1218.

(2) (a) George, S. J.; Ajayaghosh, A. *Chem.−Eur. J.* **2005**, *11*, 3217−3227 and references therein. (b) Ajayaghosh, A.; Chithra, P.; Varghese, R. *Angew. Chem., Int. Ed.* **2007**, *46*, 230−233. (c) Zhang, X.; Chen, Z.; Wurthner, F. *J. Am. Chem. Soc.* **2007**, *129*, 4886−4887. (d) Boerakker, M. J.; Botterhuis, N. E.; Bomans, P. H. H.; Frederik, P. M.; Meijer, E. M.; Nolte, R. J. M.; Sommerdijk, N. A. J. M. *Chem.−Eur. J.* **2006**, *12*, 6071−6080.

(3) (a) Aldred, M. P.; Eastwood, B.; Kelly, S. M.; Vlachos, P.; Contoret, A. E. A.; Farrar, S. R.; Mansoor, B.; O'Neill, M.; Tsoi, W. C. *Chem. Mater.* **2004**, *16*, 4928−4936. (b) O'Neill, M.; Kelly, S. M. *Adv. Mater.* **2003**, *15*, 1135−1146.

(4) (a) Schmidt-Mende, L.; Fechtenkotter, A.; Mullen, K.; Moons, E.; Friend, R. H.; Mack-enzie, J. D. *Science* **2001**, *293*, 1119−1122. (b) Kudo, W.; Kambe, S.; Nakade, S.; Kitamura, T.; Hanabusa, K.; Wada, Y.; Yanagida, S. *J. Phys. Chem. B* **2003**, *107*, 4374−4381.

(5) (a) Dai, H.; Chen, Q.; Qin, H.; Guan, Y.; Shen, D.; Hua, Y.; Tang, Y.; Xu, J. *Macromolecules* **2006**, *39*, 6584−6589. (b) Ramanan, R. M. K.; Chellamuthu, P.; Tang, L.; Nguyen, K. T. *Biotechnol. Prog.* **2006**, *22*, 118−125.

(6) (a) Kuroiwa, K.; Shibata, T.; Takada, A.; Nemoto, N.; Kimizuka, N. *J. Am. Chem. Soc.* **2004**, *126*, 2016−2021. (b) Suzuki, T.; Shinkai, S.; Sada, K. *Adv. Mater.* **2006**, *18*, 1043−1046. (c) Shklyarevskiy, I. O.; Jonkheijm, P.; Christianen, P. C. M.; Schenning, A. P. H. J.; Meijer, E. W.; Henze, O.; Kilbinger, A. F. M.; Feast, W. J.; Del Guerzo, A.; Desvergne, J.-P.; Maan, J. C. *J. Am. Chem. Soc.* **2005**, *127*, 1112−1113.

(7) (a) Murata, K.; Aoki, M.; Nishi, T.; Ikeda, A.; Shinkai, S. *J. Chem. Soc., Chem. Commun.* **1991**, 1715−1718. (b) Murata, K.; Aoki, M.; Suzuki, T.; Harada, T.; Kawabata, H.; Komori, T.; Ohseto, F.; Ueda, K.; Shinkai, S. *J. Am. Chem. Soc.* **1994**, *116*, 6664−6676. (c) Ahmed, S. A.; Sallenave, X.; Fages, F.; Mieden-Gundert, G.; Müller, U.; Vögtle, F.; Pozzo, J. L. *Langmuir* **2002**, *18*, 7096−7101. (d) Miljanic, S.; Frkanec, L.; Meic, Z.; Žinić, M. *Langmuir* **2005**, *21*, 2754−2760. (e) Koumura, N.; Kudo, M.; Tamaoki, N. *Langmuir* **2004**, *20*, 9897−9900.

(8) Naota, T.; Koori, H. *J. Am. Chem. Soc.* **2005**, *127*, 9324−9325.

(9) (a) Kawano, S. I.; Fujita, N.; Shinkai, S. *J. Am. Chem. Soc.* **2004**, *126*, 8592−8593. (b) Wang, C.; Zhang, D. Q.; Zhu, D. B. *J. Am. Chem. Soc.* **2005**, *127*, 16373−16374.

(10) Wang, C.; Robertson, A.; Weiss, R. G. *Langmuir* **2003**, *19*, 1036−1046.

(11) Aggeli, A.; Bell, M.; Boden, N.; Keen, J. N.; Knowles, P. F.; McLeish, T. C. B.; Pitkeathly, M.; Radford, S. E. *Nature* **1997**, *386*, 259−262.

(12) Varghese, R.; George, S. J.; Ajayaghosh, A. *Chem. Commun* **2005**, 593−595.

(13) Frkanec, L.; Jokic, M.; Makarevic, J.; Wolsperger, K.; Žinić, M. *J. Am. Chem. Soc.* **2002**, *124*, 9716−9717.

(14) (a) Van der Laan, S.; Feringa, B. L.; Kellogg, R. M.; Van, Esch, J. *Langmuir* **2002**, *18*, 7136−7140. (b) Koumura, N.; Kudo, M.; Tamaoki, N. *Langmuir* **2004**, *20*, 9897−9900. (c) Yagai, S.; Nakajima, T.; Kishikawa, K.; Kohmoto, S.; Karatso, T.; Kitamura, A. *J. Am. Chem. Soc.* **2005**, *127*, 11134−11139. (d) Guerzo, A. D.; Olive, A. G. L.; Reichwagen, J.; Hopf, H.; Desvergne, J.-P. *J. Am. Chem. Soc.* **2005**, *127*, 17984−17985.

(15) (a) de Loos, M.; van Esch, J.; Kellogg, R. M.; Feringa, B. L. *Angew. Chem., Int. Ed.* **2001**, *40*, 613−616. (b) De Jong, J. J. D.; Ralph Hania, P.; Pugžlys, A.; Lucas, L. N.; De Loos, M.; Kellogg, R. M.; Feringa, B. L.; Duppen, K.; Van Esch, J. H. *Angew. Chem., Int. Ed.* **2005**, *44*, 2373−2376.

(16) (a) Irie, M. *Chem. Rev.* **2000**, *100*, 1685−1716. (b) Tian, H.; Yang, S. J. *Chem. Soc. Rev.* **2004**, *33*, 85−97 and the references cited therein.

(17) (a) Li, Y.; Liu, K.; Liu, J.; Peng, J.; Feng, X.; Fang, Y. *Langmuir* **2006**, *22*, 7016−7020. (b) George, M.; Weiss, R. G. *Langmuir* **2002**, *18*, 7124−7135.

(18) Sugiyasu, K.; Fujita, N.; Takeuchi, M.; Yamada, S.; Shinkai, S. *Org. Biomol. Chem.* **2003**, *1*, 895−899.

(19) Wang, S.; Shen, W.; Feng, Y. L.; Tian, H. *Chem. Commun.* **2006**, 1497−1499.

10.1021/la7005919 CCC: $37.00
Published on Web 06/20/2007

Scheme 1. Synthesis Route and Chemical Structure of Compounds 1a, 1b, and 1c[a]

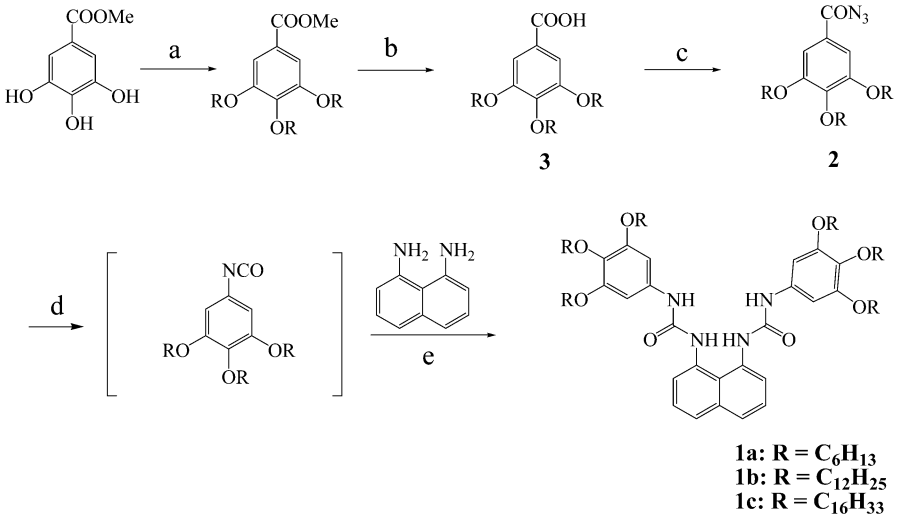

[a] Reagents and conditions: (a) RBr, K_2CO_3, KI, acetone, reflux; (b) NaOH, ethanol, HCl; (c) $SOCl_2$, NaN_3, THF; (d) Curtius rearrangement; (e) THF, reflux.

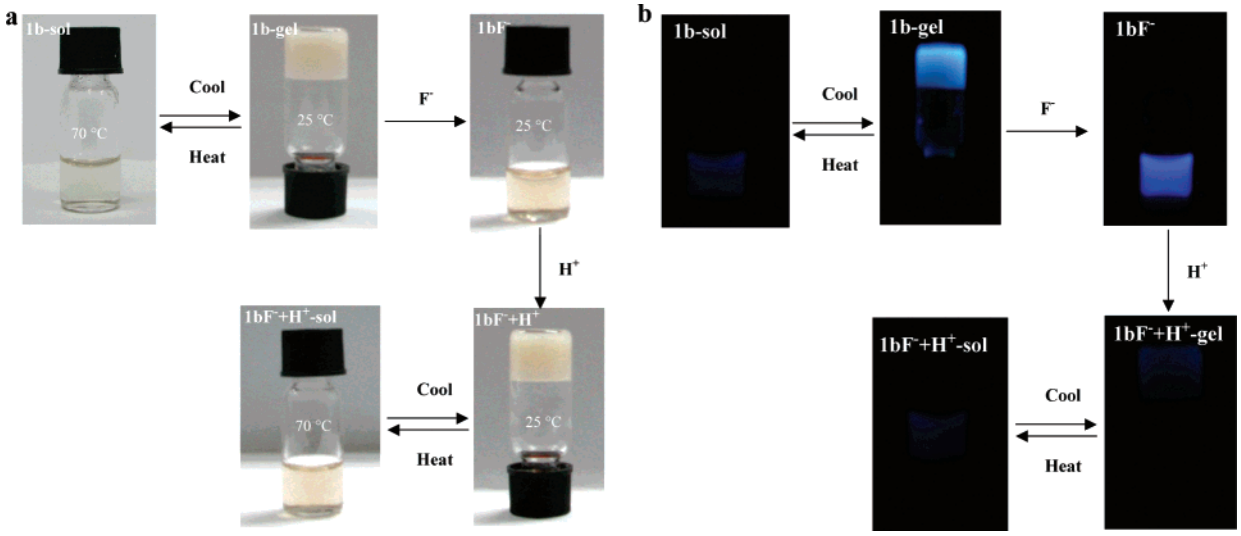

Figure 1. Images of the multiple switching process (a) and fluorescent change (b) of **1b** under the alternate effects of temperature, fluoride anions, and protons.

color change in response to external physical and chemical stimuli.[20] However, spectroscopic property changes of organogels by chemical stimuli were still limited.

As one type of important receptor, urea groups have been widely adapted as fluorescent receptors of anion sensors on the basis of the hydrogen-bonding mechanism.[21] Very recently, Zhang et al. reported a chiral gelator based on binaphthalene with two urea moieties whose circular dichroism (CD) spectra can be modified by gel formation.[22] We also reported a naphthalene derivative with bisurea for metal ion recognition.[23] In this paper, we extend our results from solutions to quasi-solid self-assembly systems. Herein, we design new naphthalene derivatives **1a**, **1b**, and **1c** consisting of bisurea and six long alkyl chains (Scheme 1) to develop switchable fluorescent organogel systems by the cooperation of intermolecular hydrogen bonding and $\pi-\pi$ interaction. We found that the sol−gel process and fluorescence of the systems could be controlled by alternate addition of fluoride anions and protons (Figure 1).

Results and Discussion

Gelation Behavior of Compounds 1a−1c. The gelation properties of **1a−1c** were evaluated in various polar and apolar, protic and nonprotic solvents. Upon cooling of the homogeneous fluid mixture of **1 (a−c)** and the solvent below the gelation temperature (T_g), the complete volume is immobilized and can support its own weight. **1b** and **1c** have similar gelation properties and are capable of gelating 10 solvents tested herein, while **1a** has a poor solubility and gelation capability in those solvents. The organogels of **1b** are very stable for months and exhibit thermally reversible sol−gel transitions. The data of the critical gelation concentration and gel to sol transition temperature (T_g) for different solvents of these compounds are shown in Table 1.

Morphologies of the Xerogels. To obtain visual images of the assembly of **1b** from various organic solvents, the morphology of the xerogels of **1b** was investigated by scanning electron microscopy (SEM). The SEM images of the *n*-hexane xerogel (Figure 2a,b) show that the gel has fibrous aggregation with

(20) Kishimura, A.; Yamashita, T.; Aida, T. *J. Am. Chem. Soc.* **2005**, *127*, 179−183.
(21) Cho, E. J.; Moon, J. W.; Ko, S. W.; Lee, J. Y.; Kim, S. K.; Yoon, J.; Nam, K. C. *J. Am. Chem. Soc.* **2003**, *125*, 12376−12377.
(22) Wang, C.; Zhang, D.; Zhu, D. *Langmuir* **2007**, *23*, 1478−1482.
(23) Yang, H.; Liu, Z. Q.; Zhou, Z. G.; Shi, E. X.; Li, F. Y.; Du, Y. K.; Yi, T.; Huang, C. H. *Tetrahedron Lett.* **2006**, *47*, 2911−2914.

Table 1. Gelation Properties of 1a, 1b, and 1c[a]

	1a			1b			1c		
solvent	state	CGC (mg/mL)	T_g (°C)	state	CGC (mg/mL)	T_g (°C)	state	CGC (mg/mL)	T_g (°C)
ethanol	I			I			I		
acetone	I			G	15	42	G	17	40
ethyl acetate	G	16	50	G	20	53	G	18	45
dimethylformamide	G	28	55	G	30	50	G	30	50
chloroform	I			G	25	48	G	23	45
xylene	G	20	50	G	25	46	G	23	48
dimethyl sulfoxide	PG			G	35	55	PG		
hexane	I			G	10	43	G	12	45
1-butanol	G	18	52	G	15	55	G	15	55
tetrahydrofuran	S			S			S		
cyclohexane	I			G	10	44	G	11	43
1,4-dioxane	G	20	50	G	20	50	G	18	50

[a] CGC = critical gelation concentration, the minimum concentration necessary for gelation of solvents, I = insoluble, S = solution when heated, G = gel, and PG = partial gel.

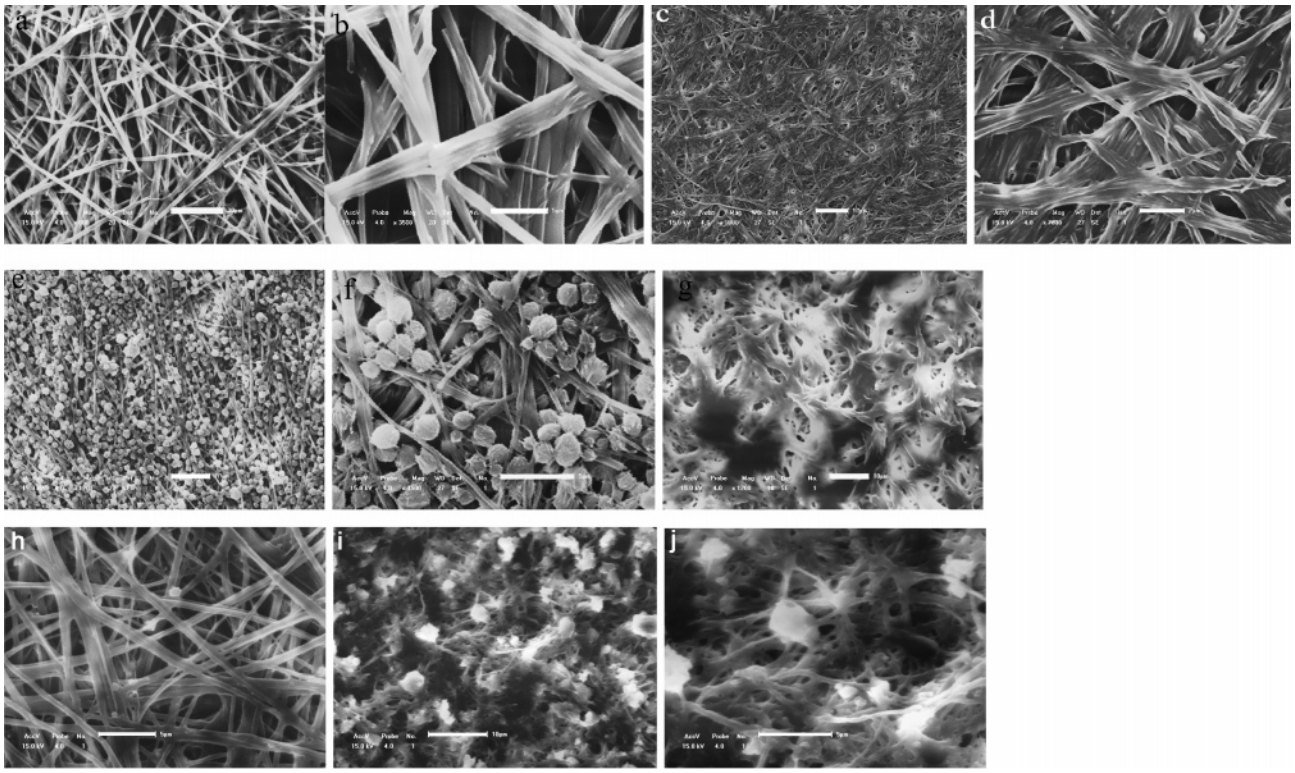

Figure 2. SEM images of the xerogels of **1b** from *n*-hexane (a, b, scale bar 20 and 5 μm, 10 mg/mL), 1-BuOH (c, d, scale bar 10 and 2 μm, 15 mg/mL), 1,4-dioxane (e, f, scale bar 10 and 5 μm, 20 mg/mL), **1b**F^-+H^+ gel from 1,4-dioxane (g, scale bar 10 μm, 20 mg/mL), **1a** from 1,4-dioxane (h, scale bar 5 μm, 20 mg/mL), and **1c** from 1,4-dioxane (i, j, scale bar 10 and 5 μm, 20 mg/mL).

diameters of ~0.5−2.5 μm. The xerogel from 1-BuOH has a smooth belt structure with the width of the belt in the range of 0.4−2.0 μm (Figure 2c,d). In 1,4-dioxane, it is interesting that the gel shows regular wool balls about 0.5−1.5 μm in size, connected by thin ribbons (Figure 2e,f). The morphology of the xerogels from **1a** and **1c** in 1,4-dioxane was also measured and is shown in parts h and parts i and j, respectively, of Figure 2. Different with **1b** from the same solvent, **1a** has a smooth belt structure with the width of the belt in the range of 0.4−1.0 μm. The longer alkyl chain compound **1c** gives an image much more like that of **1b**, with the balls connected by thin ribbons. On the basis of the above results, we can see that the morphology of the xerogels depends on the length of the alkyl chain and the nature of the gelling solvents. The solvent-tunable morphology in an azobenzene gelator with several competition or cooperative interactions has been described in our group work.[24] This feature most likely results from a strongly anisotropic growth. The process is related to highly directional intermolecular interactions that in turn may be due to the partial or full extension of the long alkyl chains or to the formation of directional molecular aggregates.

Temperature-Induced Fluorescent Change in the Gel States. Fluorescence spectra are frequently sensitive to the microenvironment around the fluorescent probe. All three compounds **1a**−**1c** have similar emission properties. They show quite different fluorescence spectra between the solution and the gel state. Herein, we typically discuss the fluorescent properties of **1b** in detail; the spectral data of **1a** and **1c** are in the Supporting Information. As shown in Figure 3a, **1b** in the dilute solution

(24) Zhou, Y. F.; Yi, T.; Li, T. C.; Zhou, Z. G.; Li, F. Y.; Huang, W.; Huang, C. H. *Chem. Mater*. **2006**, *18*, 2974−2981.

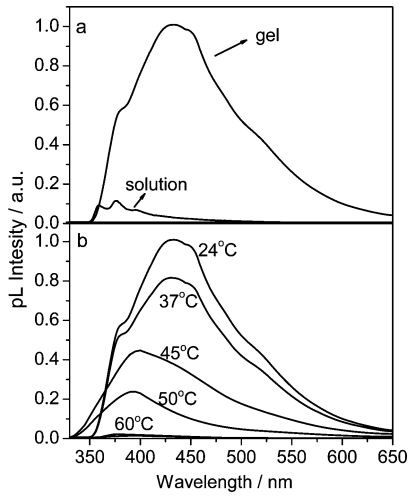

Figure 3. (a) Fluorescence spectra of **1b** in 1,4-dioxane solution (1.0×10^{-4} mol·L^{-1}) and in the gel phase (22 mg/mL) at room temperature. (b) Variable-temperature fluorescence spectra of **1b** with a high concentration in 1,4-dioxane (22 mg/mL) ($\lambda_{ex} = 310$ nm).

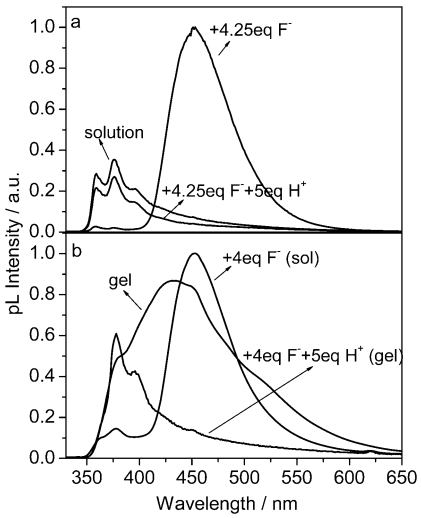

Figure 4. Fluorescence spectra of **1b** in the presence of fluoride anions and TFA, alternately, at room temperature in 1,4-dioxane: (a) in the dilute solution (1.0×10^{-4} mol·L^{-1}), (b) in a relatively highly concentrated sample (22 mg/mL) which can form a gel in its original state ($\lambda_{ex} = 310$ nm).

(1,4-dioxane, 1.0×10^{-4} mol·L^{-1}) exhibited a split structural emission band ($\lambda = 359$, 376, and 396 nm) which was attributed to the characteristic monomer emission of the naphthalene group.[25] The structureless broad emission centered at 433 nm with a shoulder peak at 376 nm was observed in the gel state (22 mg/mL in 1,4-dioxane), with an impressive increase in the photoluminescence (PL) intensity compared with that in the solution. Herein, the decrease of the fluorescent intensity in a high concentration by the inner filter effect[26] was neglected. The remarkable fluorescence enhancement from gels was unambiguously assigned to the phenomenon of aggregation-induced enhanced emission (AIEE).[27]

To confirm the effect of the fluorophore part along with the sol−gel transition, temperature-dependent fluorescence spectra of **1a**−**1c** in the 1,4-dioxane gel state were measured. Herein, **1b** is discussed in detail as an example and shown in Figure 3b. The spectra of **1a** and **1c** are given in Figures S1 and S2 of the Supporting Information. Upon heating, no obvious shift of the emission bands was observed in the gels of **1a**−**1c** below 45 °C. Nevertheless, above 45 °C, the gels turned into fluid solutions, and the emission was blue-shifted to 380 nm in **1a** and **1b** and 375 nm in **1c** along with the evident decrease of the fluorescence intensity. The temperature dependence of fluorescence spectra of **1b** in other solvents resembled that in 1,4-dioxane (see Figure S3 in the Supporting Information). These results are in line with the formation of molecular J-aggregations of the naphthalene group in which the excitonic energy is delocalized as a result of intermolecular coupling within the head-to-head arrangement of the fluorophore in the molecular packing of the gel.[28]

Fluoride Anion and Proton Response of the Gels under the Probe of Fluorescence. It was reported that the naphthalene urea derivative was selectively sensitive to fluoride anions.[21] We found that **1b** showed similar fluorescent changes under addition of tetrabutylammonium fluoride in the diluted solution (1.0×10^{-4} mol·L^{-1}) as previously reported.[21] As shown in Figures 4a and S5 (Supporting Information), when fluoride anions were added to the solution of **1b**, the characteristic fluorescent emission band of **1b** centered at 380 nm greatly decreased, and a new band centered at 450 nm increased. The intensity of the band no longer changed when the ratio of fluoride anions to **1b** reached 4.25 equiv. Even if the dual fluorescence still exists in the complex system (**1b**F$^-$), the ratio of the intensity between 450 and 380 nm is up to 30. This phenomenon was due to the interaction between bisurea and fluoride anion by strongly charged hydrogen bonding.[29] Furthermore, the **1b**F$^-$ solution is very sensitive to acid. The longer wavelength emission disappeared by addition of trifluoroacetic acid (TFA) to the solution of **1b**F$^-$. The effect of TFA$^-$ on **1b** was also investigated. We found that the position of the emission band of **1b** was not changed; only a slightly decrease of the intensity was observed in the case of the presence of 10 equiv of tetrabutylammonium trifluoroacetate (TFA$^-$) in solution (see Figure S6 in the Supporting Information), which means that **1b** is not sensitive to TFA$^-$ anions. Probably, the stronger interaction between F$^-$ and the protons of TFA could weaken the binding between F$^-$ and urea groups of **1b** and thus lead to a blue-shifted fluorescence of the **1b**F$^-$ system.

The interaction of **1a**−**1c** with fluoride anions in the gel state was also investigated in 1,4-dioxane through a fluorescent titration experiment. As shown in Figures S7−S9 (Supporting Information), when the addition of fluoride anions was less than 2 equiv of **1a**−**1c**, dual fluorescence was observed with a decrease of fluorescence at 430 nm and an increase at 380 nm. Upon further addition of the fluoride anions, the band at 380 nm decreased again and a comparatively strong and narrow peak appeared at the position of 455 nm (Figures 4b and S7−S9). The different excited states were observed for the emission of gel **1b** and sol **1b**F$^-$ (see Figures S10 and S11 in the Supporting Information). At the same time, the gel−sol transition happened along with the addition of fluoride anions for all three compounds at room temperature, and this transition process was completed in the presence of about 4 equiv of fluoride anions. The possible explanation for this phenomenon is that the formation of hydrogen bonds between four NH moieties of bisurea and fluoride anions

(25) Costa, T.; Miguel, M. D. G.; Lindman, B.; Schillen, K.; Seixas de Melo, J. S. *J. Phys. Chem. B* **2005**, *109*, 11478−11492.

(26) Andrieux, K.; Lesieur, P.; Lesieur, S.; Ollivon, M.; Grabielle-Madelmont, C. *Anal. Chem.* **2002**, *74*, 5217−5226.

(27) (a) An, B. K.; Kwon, S. K.; Jung, S. D.; Park, S. Y. *J. Am. Chem. Soc.* **2002**, *124*, 14410−14415. (b) Chen, J. W.; Law, C. C. W.; Lam, J. W. Y.; Dong, Y. P.; Lo, S. M. F.; Williams, I. D.; Zhu, D. B.; Tang, B. Z. *Chem. Mater.* **2003**, *15*, 1535−1546.

(28) Camerel, F.; Bonardi, L.; Schmutz, M.; Ziessel, R. *J. Am. Chem. Soc.* **2006**, *128*, 4548−4549.

(29) Vazquez, M.; Fabbrizzi, L.; Taglietti, A.; Pedrido, R. M.; Gonzalez-Noya, A. M.; Bermejo, M. R. *Angew. Chem., Int. Ed.* **2004**, *43*, 1962−1965.

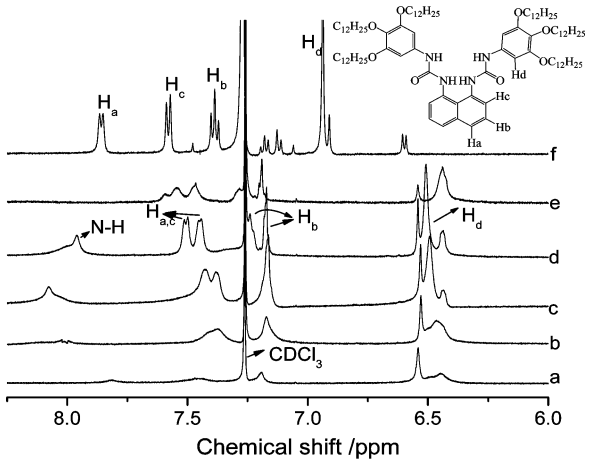

Figure 5. ^{1}H NMR spectra of **1b** (30 mg/mL) in $CDCl_3$ at different temperatures: (a) 24 °C, (b) 30 °C, (c) 40 °C, (d) 50 °C, (e) with a diluted concentration (7.6 mg/mL) at 40 °C, (f) 30 mg/mL of **1b** in the presence of 4 equiv of $(C_4H_9)_4NF$ at 24 °C.

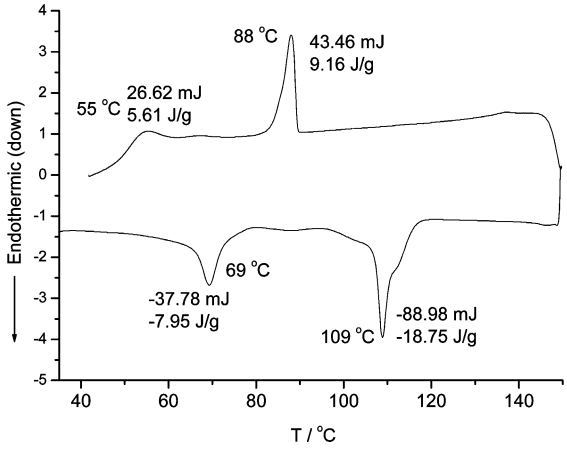

Figure 6. DSC curves of **1b** on the first heating and cooling cycles.

or the deprotonation of the urea moiety by fluoride anions[29] destroyed the intermolecular hydrogen bonds between the urea groups. As a result, the gel−sol transition happened. Other halides such as Cl^-, Br^-, and I^- have no obvious effect on the fluorescence as well as the gel−sol transition of **1a**−**1c** or **1a**F^-−**1c**F^- (see Figures S12−14 in the Supporting information).

Furthermore, the gel formation of **1a**F^-−**1c**F^- (1,4-dioxane) systems was recovered by the addition of TFA. The fluorescence spectra of **1a**F^-−**1c**F^- were measured as a function of the content of TFA at room temperature. It was seen from Figures 4b and S15−S17 (Supporting Information) that the emission at 455 nm in the **1a**F^-−**1c**F^- systems disappeared and the 380 nm emission increased upon addition of TFA, which is due to the stronger interaction between F^- and TFA. As a result, new gels of (**1a**F^-+H^+)−(**1c**F^-+H^+) with a 70 nm blue-shifted emission were obtained in the meantime. The difference between the gel **1b**F^-+H^+ and the original gel **1b** was not only in the spectral properties, but also in the morphologies of the xerogels (see the SEM images in Figure 2e,g).

To study the driving force of the gel−sol process, temperature- and concentration-dependent ^{1}HNMR spectra were examined. ^{1}H NMR spectra of **1b** (ca. 30 mg/mL in $CDCl_3$) at 24, 30, 40, and 50 °C are shown in Figure 5. The ^{1}H NMR spectrum of the aromatic protons in **1b** displayed broad signals even at elevated temperatures. H_a, H_b, and H_c went to lower field positions with increasing temperature. The proton signal of the urea groups of **1b** at 24 °C was very weak. At 40 °C, a broad signal at about 8.08 ppm assigned to the protons of the urea groups was detected. These results implied that the intermolecular H-bonds were formed between neighboring urea groups at room temperature. The intermolecular H-bonds became weaker by increasing the temperature, and as a result, the proton signal of the urea groups were shifted upfield to 7.96 ppm at 50 °C. A concentration-dependent chemical shift was also observed. The aromatic proton signals of H_a, H_b, and H_c appeared in a higher magnetic field compared to those at a dilute concentration of 7.6 mg/mL at the same temperature (40 °C) (Figure 5c,e). This chemical shift change of the aromatic protons with concentration is consistent with that of the temperature dependence, which implies $\pi-\pi$ stacking among the naphthalene core moieties.[30]

The ^{1}H NMR spectrum of **1b** was also recorded in the presence of 4.0 equiv of F^- (see Figure 5f). After the addition of F^-, the aromatic proton signals shifted downfield due to the interaction between **1b** and F^-, which disrupted the $\pi-\pi$ stacking among the naphthalene core. The amide NH signal disappeared, which may be due to the deprotonation of the urea groups by F^-. The same results were also observed in previous studies.[21,31] These results suggested that hydrogen bonds were the key point of the self-assembly.

Figure 1 shows the whole switching processes and fluorescent change with photographic images of **1b** under the cooperative effects of temperature, fluoride anions, and protons. Thus, both the sol−gel transition and fluorescent change can be controlled by tuning the temperature or introducing fluoride anions/protons. In this process, the emission is reversibly changed from a strong blue color (switch on, visible by the naked eye) in the gel state (**1b** gel) to a visible inactive emission (switch off) of the sol state (**1b** sol) by changing the temperature. The fluorescent **1b** gel can also be turned into a fluorescent sol (**1b**F^-) upon addition of the fluoride anions at room temperature and back to a visible inactive emission gel (**1b**F^-+H^+ gel, emission in the UV range) upon addition of TFA. Finally, the **1b**F^-+H^+ gel becomes a **1b**F^-+H^+ sol by increasing the temperature. This process could be repeated many times.

Behavior of the Mesophase States of the Compounds. All three compounds **1a**−**1c** were found to exhibit liquid crystalline (LC) properties in large temperature ranges. For example, on first heating of **1b** from room temperature, two endothermic peaks at 69 and 109 °C were observed in the DSC curve (Figure 6), indicating transitions from the crystalline solid phase to the LC mesophase. When the sample was cooled from 200 °C, a well-defined "square-shaped" texture developed from polarizing optical microscopy (POM; Figure 7a) at temperatures below 190 °C, and this shape changed to a branched texture (Figure 7b) below 92 °C, which was maintained till room temperature. The POM images for the gel sample of **1b** from 1,4-dioxane only showed one mesophase texture from 130 to 50 °C (Figure 7c) concomitant with a dark fibrous structure in the image. **1a** and **1c** showed LC phases from 64 to 191 °C and from 59 to 163 °C, respectively, from DSC curves (Figures S18 and S19 in the Supporting Information).

Perspective Molecular Structure of 1b. To investigate the molecular resolution and phase transition of **1b**, variable-temperature small-angle X-ray scattering (SAXS) was performed, and the patterns are shown in Figure 8. The SAXS patterns of the powder prepared at different temperature show the different series of reflections. At 25 °C, the observed spacings of 38.4

(30) Ishi-i, T.; Hirayama, T.; Murakami, K.-i.; Tashiro, H.; Thiemann, T.; Kubo, K.; Mori, A.; Yamasaki, S.; Akao, T.; Tsuboyama, A.; Mukaide, T.; Ueno, K.; Mataka, S. *Langmuir* **2005**, *21*, 1261−1268.

(31) Lee, J. Y.; Cho, E. J.; Mukamel, S.; Nam, K. C. *J. Org. Chem.* **2004**, *69*, 943−950.

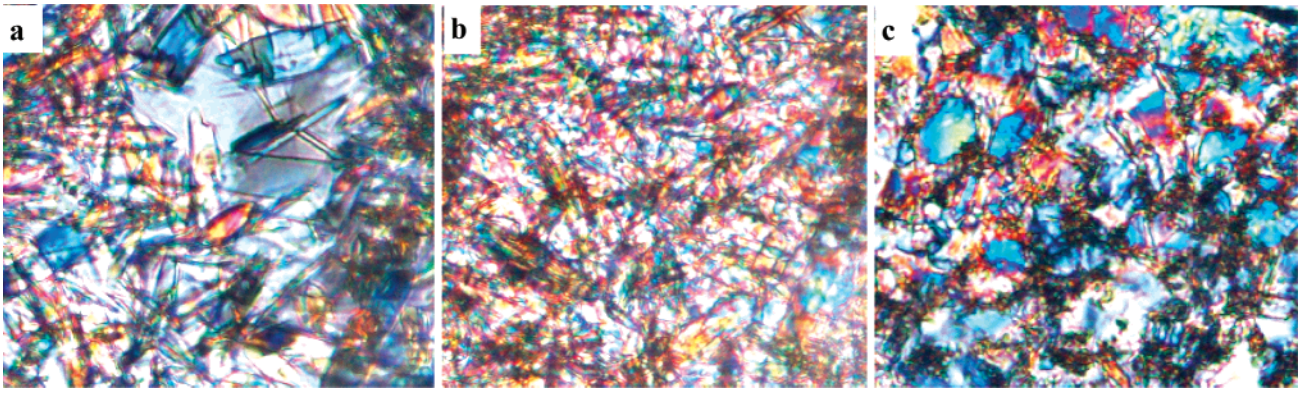

Figure 7. Polarizing optical micrographs of **1b** in the solid state on first cooling at temperatures of 147 (a) and 85 (b) °C and in the gel state (22 mg/mL) on first cooling at a temperature of 94 °C (c) (magnification 200×).

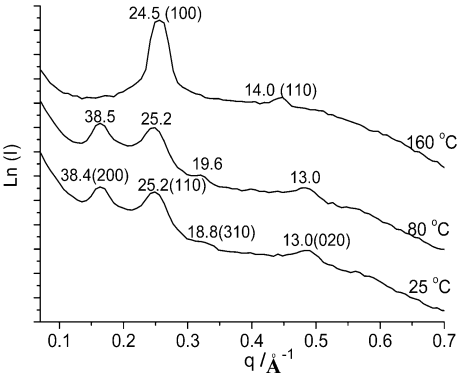

Figure 8. Variable-temperature SAXS patterns of **1b**.

(200), 25.2 (110), 18.8 (310), and 13.0 (020) Å form a suite of fractions, strongly suggesting a column (Col_r) structure with structure parameters of $a = 76.8$ Å and $b = 26.0$ Å. When the sample was heated from room temperature to 80 °C, there was no obvious change in the measured angle region corresponding to *d* values of 38.4 and 13.0 Å; only the diffraction was more distinct with a *d* value of 19.6 Å. When it was further heated to 160 °C, three original diffractions disappeared and another series of reflections appeared. *d* spacings of 24.5 (100) and 14.0 (110) Å showed the formation of a Col_h structure with a structure parameter of $a = 28.3$ Å.

According to the structure parameter and CPK molecular modeling of **1b**, the molecular packing model of **1b** at room temperature was conjectured and is shown in Figure 9. The monomers are connected by both double hydrogen bonds between ureas and $\pi\cdots\pi$ interaction of the naphthalene group to form a one-dimensional arrangement (Figure 9a). The urea part was located at the center of the packing and formed the intermolecular hydrogen bonds in the *c* direction. The long structure parameter of the packing of **1b** (Col_r) indicates that the two molecules along the *a* direction are entwisted by six long alkyl chains to form a dimer as shown in Figure 9b. Thus, the dimers arranged as a one-dimensional column structure by intermolecular hydrogen bonds cooperating with $\pi\cdots\pi$ interaction of the naphthalene group (Figure 9c). The strong interaction between fluoride anions and urea groups weakens the intermolecular interaction of the gel and thus results in damage of the gel state (Figure 9d). The sol state of **1b**F^- can be reversed to the gel state by addition of protons. Both the emission properties and the morphology of the newly produced gel are quite different from those of the original one, which means that the addition of TFA disturbs the intermolecular hydrogen bonds and the packing of fluorophores between molecules of **1b** and may contribute to the formation of the new gel state.

Conclusions

In conclusion, we present an effective approach to fluorescent organogel systems, which are sensitive to temperature, fluoride anions, and protons. The cooperation of hydrogen bonds and $\pi-\pi$ stacking interaction of the fluorophore plays a crucial role in the formation of the organogels. The fluorescent emission is strongly dependent on the aggregation of the fluorophore and therefore very sensitive to a change of the chemical environment. A stronger and red-shifted emission was found in the gel state or under addition of fluoride anions compared with that of the original solution. The gel−sol transition of the systems, as well as the fluorescent emission, is reversibly controlled by a change of the temperature or upon alternative addition of fluoride anions and protons.

Experiment Section

General Procedures. All starting materials were obtained from commercial suppliers and used as received. Moisture-sensitive reactions were performed under an atmosphere of dry argon. ^{1}H NMR and ^{13}C NMR spectra were recorded on a Mercury plus, 400 and 100 MHz, respectively. The temperature-dependent ^{1}H NMR spectra were recorded with a Bruker 500 MHz spectrameter. Proton chemical shifts are reported in parts per million downfield from tetramethylsilane (TMS). UV−vis spectra were recorded on a UV−vis 2550 spectroscope (Shimadzu). The luminescence spectra were measured on an Edinburgh LFS920 fluorescence spectrophotometer (the path length of the quartz cell is 1 cm). SEM images of the xerogels were obtained using an SSX-550 (Shimadzu) with an accelerating voltage of 15 kV. Samples were prepared by spinning the gels on glass slices and coating with Au. SAXS diagrams were obtained on a NanoSTAR U SAXS system (Bruker), using a Cu Kα radiation source ($\lambda = 0.1542$ nm). The SAXS data were corrected for absorption and background scattering. Liquid crystal photos were recorded on an LV100POL (Nikon Corp.) polar optical microscope equipped with a hot stage. Elementary analysis data were obtained on an Elementar vario EL III (Germany).

The titration test was carried out as follows: the gelator **1b** (22 mg) was mixed in a capped quartz optical cell with 1 mL of 1, 4-dioxane, and the mixture was heated until the solid was dissolved. The sample cell was cooled to room temperature in air until a stable gel formed. The gel sample was then heated again and kept at 70 °C to turn to the sol state. To this sol sample were added different amounts of fluoride anions (tetrabutylammonium fluoride), and the resulting sol was left for 30 min at this temperature and then cooled to room temperature. The fluorescence spectrum was measured at both 70 °C and room temperature. Control experiments were also carried out. The gel could turn to the sol state by addition of fluoride anions at room temperature, but the transition from gel to sol was not observed by adding an equivolume of solvent only.

Synthesis and Characterization. **1a**, **1b**, and **1c** were synthesized in a similar process. Here, the synthesis of **1b** is described in detail as follows.

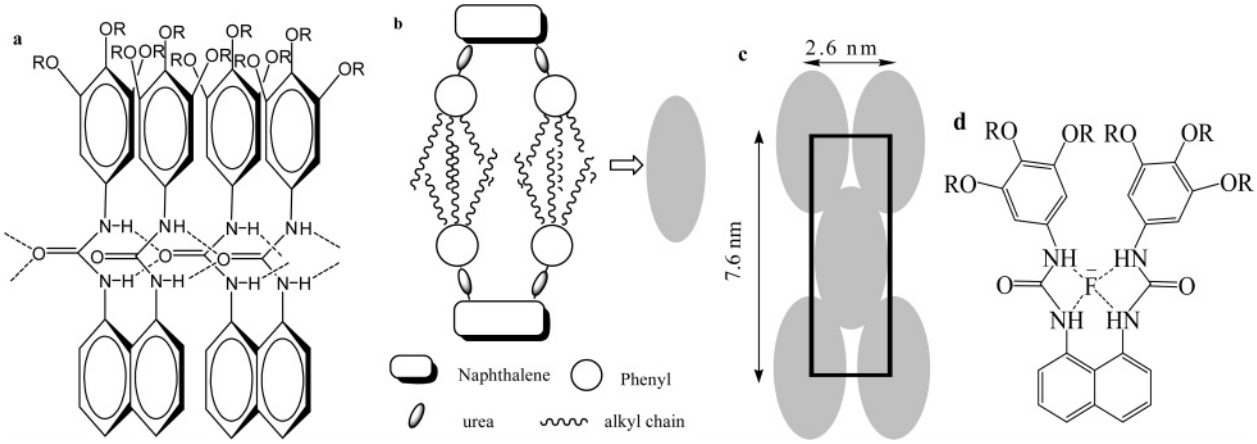

Figure 9. Expected model of the intermolecular hydrogen bonds (a), hydrophobic interaction (b), packing structure in Col_r (c), and interaction with fluoride anions (d) in **1b**.

*3,4,5-Tris(dodecyloxy)benzoic Acid (**3b**)*. White solid **3b** was synthesized according to a previous report.[32] To 150 mL of dry acetone solution containing 3,4,5-trihydroxybenzoic acid methyl ester (1.84 g, 10 mmol) and 3.5-fold dodecyl bromide (8.72 g, 35 mmol) were added 5.56 g (40 mmol) of anhydrous potassium carbonate and a small amount of potassium iodide. The reaction mixture was refluxed and stirred for 2 days. The solution was then evaporated to dryness and partitioned between dichloromethane (50 mL) and water (50 mL). The combined organic phases were dried, filtered, and evaporated to give a colorless oil, which was recrystallized with ethanol. The resulting white solid was filtered, dried under vacuum, dissolved in a mixture of ethanol (60 mL) and 20 mL of 0.5 M KOH solution, and refluxed for 6 h. Neutralization until pH 1 with 1 M hydrochloric acid provided a white precipitate, which was separated by filtration. Recrystallization from hot ethanol gave 4 g (yield 60%) of **3b** as a white solid.

*3,4,5-Tris(dodecyloxy)benzoyl Azide (**2b**)*. A 5 mL portion of $SOCl_2$ (excess) was dropped into 10 mL of a THF solution of **3** (3.4 g, 5 mmol). The reaction mixture was refluxed and stirred for 4 h, and then the solvent and excess $SOCl_2$ were evaporated under reduced pressure. The resulting 4-[(4-alkoxyphenyl)azo]benzoyl chloride was then dissolved in 10 mL of THF and dropped into 50 mL of an aqueous solution of NaN_3 (3.25 g, 50 mmol) in an ice bath. The reaction mixture was stirred overnight. The precipitate was filtered, and the crude product was obtained as a yellow solid. The crude product was purified by column chromatography on silica gel with acetic ester/petrol ether (1:5, v/v) as the eluent, giving a 75% yield of **2b**: ^{1}H NMR ($CDCl_3$, 25 °C) δ 7.24 (ArH, 2H), 4.05−4.03 (t, J = 5.2 Hz, $-OCH_2CH_2-$, 2H), 4.02−3.99 (t, J = 5.2 Hz, $-OCH_2$-CH_2-, 4H), 1.84−1.78 (m, $-OCH_2CH_2-$, 4H), 1.76−1.71 (m, $-OCH_2CH_2-$, 2H), 1.34−1.26 (m, $-CH_2-$, 54H), 0.89−0.87 (t, J = 5.4 Hz, $-CH_3$, 9H); ^{13}C NMR ($CDCl_3$, 25 °C) δ 171.9, 153.0, 144.0, 125.1, 108.0, 73.6, 69.3, 31.9, 29.7, 29.6, 29.6, 29.5, 29.4, 29.3, 26.1, 22.7, 14.1.

*Data for **2a***: 85% yield; ^{1}H NMR ($CDCl_3$, 25 °C) δ 7.24 (ArH, 2H), 4.06−4.02 (t, J = 8.0 Hz, $-OCH_2CH_2-$, 2H), 4.02−3.98 (t, J = 8.0 Hz, $-OCH_2CH_2-$, 4H), 1.83−1.78 (m, $-OCH_2CH_2-$, 4H), 1.76−1.70 (m, $-OCH_2CH_2-$, 2H), 1.50−1.32 (m, $-CH_2-$, 18H), 0.89−0.91 (t, J = 4.0 Hz, $-CH_3$, 9H); IR (KBr) ν (cm^{-1}) 2926 (CH_3), 2137 (CON_3), 1200 (N_3).

*Data for **2c***: 70% yield; ^{1}H NMR ($CDCl_3$, 25 °C) δ 7.24 (ArH, 2H), 4.05−4.01 (t, J = 8.0 Hz, $-OCH_2CH_2-$, 2H), 3.97−3.94 (t, J = 8.0 Hz, $-OCH_2CH_2-$, 2H), 3.96−3.92 (t, J = 8.0 Hz, $-OCH_2$-CH_2-, 2H), 1.83−1.71 (m, $-OCH_2CH_2-$, 6H), 1.50−1.32 (m, $-CH_2-$, 78H), 0.90−0.86 (t, J = 8.0 Hz, $-CH_3$, 9H); IR (KBr) ν (cm^{-1}) 2913 (CH_3), 2156 (CON_3), 1212 (N_3).

*1-[3,4,5-Tris(dodecyloxy)phenyl]-3-{8-[3-[3,4,5-tris(dodecyloxy)-phenyl]ureido]naphthalen-1-yl}urea (**1b**)*. **1b** was easily synthesized according to the reported procedure,[28] in which **2b** produced the isocyanate derivative upon heating (Curtius rearrangement), which in turn reacted with the diaminonaphthalene to give compound **1b**. To a solution of 1,8-diaminonaphthalene (0.09 g, 0.6 mmol) in 10 mL of CH_2Cl_2 was added 10 mL of a CH_2Cl_2 solution of **2b** (1.0 g, 1.4 mmol) dropwise over 30 min. The reactant was refluxed for 6 h in a nitrogen atmosphere. Then the solid product was filtered and washed with CH_2Cl_2 to give 0.72 g of white solid powder **1b**: 80% yield; ^{1}H NMR (mixture of DMSO-d_6/$CDCl_3$ (1:1, v/v), 60 °C) δ 8.59−8.57 (ArH, 4H), 7.64−7.60 (ArH, 4H), 7.39−7.36 (ArH, 2H), 6.67 (s, NH, 2H), 6.61 (s, NH, 2H), 3.75−3.72 (t, J = 6.4 Hz, $-OCH_2CH_2-$, 4H), 3.90−3.87 (t, J = 6.4 Hz, $-OCH_2CH_2-$, 8H), 1.72−1.59 (m, $-OCH_2CH_2-$, 12H), 1.42−1.39 (m, $-CH_2CH_3$, 12H), 1.26−1.23 (m, $-CH_2-$, 96H), 0.85−0.81 (t, J = 6.4 Hz, $-CH_3$, 18H). Anal. Calcd for $C_{96}H_{164}N_4O_8$: C, 76.75; H, 11.00; N, 3.73; Found: C, 76.47; H, 11.09; N, 3.69.

*Data for **1a***: white solid powder; 75% yield; ^{1}H NMR (mixture of DMSO-d_6/$CDCl_3$ (2:1, v/v), 25 °C) δ 7.17−7.13 (ArH, 6H), 7.06−7.04 (ArH, 4H), 6.49 (s, NH, 2H), 6.47 (s, NH, 2H), 3.87−3.78 (m, -OCH_2CH_2-, 12H), 1.87−1.85 (m, $-OCH_2CH_2-$, 12H), 1.44−1.35 (m, $-CH_2CH_3$, 12H), 1.28−1.22 (m, $-CH_2-$, 24H), 0.83−0.85 ($-CH_3$, 18H). Anal. Calcd for $C_{60}H_{92}N_4O_8$: C, 72.25; H, 9.30; N, 5.62; Found: C, 72.05; H, 9.35; N, 5.55.

*Data for **1c***: white solid powder; 68% yield; ^{1}H NMR (mixture of DMSO-d_6/$CDCl_3$ (2:1, v/v), 25 °C) δ 7.16−7.09 (ArH, 4H), 7.04−7.02 (ArH, 4H), 6.88−6.94 (ArH, 2H), 6.48 (s, NH, 2H), 6.46 (s, NH, 2H), 3.92−4.00 (m, $-OCH_2CH_2-$, 12H), 1.94−1.87 (m, $-OCH_2CH_2-$, 12H), 1.72−1.68 (m, $-CH_2CH_3$, 12H), 1.19−1.15 (m, $-CH_2-$, 144H), 0.83−0.85 ($-CH_3$, 18H). Anal. Calcd for $C_{120}H_{212}N_4O_8$: C, 78.37; H, 11.62; N, 3.05; Found: C, 78.07; H, 11.44; N, 3.20.

Acknowledgment. We thank the National Science Foundation of China (Grants 20490210, 20501006, and 20571016) and Shanghai Science and Technology Committee (Grants 05DJ14004, 06QH14002, and 06PJ14016) for financial support.

Supporting Information Available: Emission and absorption spectra of **1a**−**1c** in the solution and gel states. This material is available free of charge via the Internet at http://pubs.acs.org.

LA7005919

(32) Terazzi, E.; Torelli, S.; Bernardinelli, G.; Rivera, J. P.; Benech, J. M.; Bourgogne, C.; Donnio, B.; Guillon, D.; Imbert, D.; Bunzli, J. C. G.; Pinto, A.; Jeannerat, D.; Piguet, C. *J. Am. Chem. Soc.* **2005**, *127*, 888−903.